Thermal acclimation of photosynthetic activity and Rubisco content in two hybrid poplar clones

Lahcen Benomar[*1]., Mohamed.Taha Moutaoufik [2]., Raed Elferjani[3]., Nathalie Isabel[4]., Annie DesRochers[5]., Ahmed El Guellab[1]., Rim Khlifa[6]., Lala Amina Idrissi Hassania [7].

[1] Faculté de foresterie, de géographie et de géomatique, Pavillon Abitibi Price, Université Laval, Québec, Québec G1V 0A6, Canada

[2] Department of Biochemistry, University of Regina, Regina, Saskatchewan S4S 0A2, Canada

[3] Saskatoon Research and Development Centre, Agriculture and Agri-Food Canada, 107 Science Place, Saskatoon, Saskatchewan S7N 0X2, Canada

[4] Natural Resources Canada, Canadian Forest Service, Laurentian Forestry Centre, 1055 du P.E.P.S, PO Box 10380, Stn. Sainte-Foy, Quebec, QC G1V 4C7, Canada

[5] Université du Québec en Abitibi-Témiscamingue, 341 Principale Nord, Amos, Québec J9T 2L8, Canada

[6] Centre d'étude de la forêt, Département des sciences biologiques, Université du Québec à Montréal, Montréal, Québec H3C 3P8, Canada

[7] Laboratoire de Biotechnologies végétales, Équipe Planta sud, Faculté des Sciences, Université Ibn Zohr Agadir, Morocco.

*** Corresponding author:**
lahcen.benomar.1@gmail.com (LB)

Abstract

The mechanistic bases of thermal acclimation of net photosynthetic rate (A_n) are still difficult to discern and empirical research remains limited, particularly for hybrid poplar. In the present study, we examined the contribution of a number of biochemical and biophysical traits on thermal acclimation of A_n for two hybrid poplar clones. We grew cuttings of *Populus maximowiczii* × *Populus nigra* (M×N) and *Populus maximowiczii* × *Populus balsamifera* (M×B) clones under two day/night temperature of 23°C/18°C and 33°C /27°C and under low and high soil nitrogen level. After 10 weeks, we measured leaf RuBisCO and RuBisCO activase (*RCA*) amounts and the temperature response of A_n, dark respiration (R_d), stomatal conductance, (g_s), maximum carboxylation rate of CO_2 (V_{cmax}) and photosynthetic electron transport rate (J). Results showed that a 10°C increase in growth temperature resulted in a shift in thermal optimum (T_{opt}) of A_n of 6.2±1.6 °C and 8.0±1.2 °C for clone M×B and M×N respectively, and an increased A_n and g_s at the growth temperature for clone M×B but not M×N. RuBisCO amount was increased by N level but was insensitive to growth temperature while *RCA* amount and the ratio of its short to long isoform was stimulated by warm condition for clone M×N and at low N for clone M×B. The activation energy of V_{cmax} and J decreased under warm condition for clone M×B and remain unchanged for clone M×N. Our study demonstrated the involvement of both *RCA*, activation energy of V_{cmax} and stomatal conductance in thermal acclimation of A_n.

Introduction

Global warming may lead to a significant reduction of forest productivity through a decrease in net assimilation rate of CO_2 (Lloyd and Farquhar, 2008; Sage et al., 2008). Plant physiological processes including light-saturated photosynthetic rate (A_n) and dark respiration (R_d) are strongly temperature-dependent and their acclimation may help trees maintain a normal growth when temperature shifts from optimum to warm (Atkin et al., 2005; Medlyn et al., 2002; Sage et al., 2008). Thermal acclimation of A_n is achieved through adjustments of one or more morphological, biochemical and biophysical components of photosynthesis which may occur via (i) a shift of the thermal optimum of A_n (T_{opt}) toward the new growth temperature (ii) an increase or a maintenance of the photosynthetic rate at T_{opt} (A_{opt}) at warmer growth temperatures (iii) a shift in both A_{opt} and T_{opt}, and (iv) an increase or a maintenance of the photosynthetic rate respective to growth temperature (A_{growth}) (Sage and Kubien, 2007; Way and Yamori, 2014; Yamori et al., 2014). The mechanisms involved in thermal acclimation of photosynthesis are still difficult to discern and may originate, among others, from species thermal origin (Yamori et al., 2009). They include modulation of (i) basal maximum carboxylation rate V_{cmax}^{25} or maximum electron transport rate J_{max}^{25} (measured at reference temperature of 25°C), (ii) thermal response of both V_{cmax} and J_{max} (activation and deactivation energy), (iii) nitrogen allocation to carboxylation *vs.* elctron transport (ratio of J_{max} to V_{cmax}) and (iv) thermal response of stomatal and mesophyll conductance (Hikosaka et al., 2006; Sage and Kubien, 2007; Way and Yamori, 2014; Yamori et al., 2014).

Leaf nitrogen (N) plays a key role in carbon assimilation processes and hence plant growth and survival (DesRochers et al., 2003; Fisichelli et al., 2015), as most of the leaf nitrogen is allocated to proteins involved in light harvesting, Calvin-Benson cycle and electron transfer along thylakoid membranes (Field, 1983; Poorter et al., 2009). Leaf nitrogen content is generally deficient in temperate and boreal regions and has been shown to decrease in response to increasing growth temperature (Reich and Oleksyn, 2004; Gunderson et al., 2010; Scafaro et al., 2016). A decrease in leaf N in response to increasing growth temperature may result in a decrease of RuBisCO content (Scafaro et al., 2016). This has been proposed as an explanation of the commonly observed deacrease in V_{cmax} at temperatures above the optimum and the resulting lack of thermal acclimation of A_n (Scafaro et al., 2016; Crous et al., 2018). On the other hand, Yamori et al., (2011) found that photosynthesis temperature response of several C_3 plants was generally RuBP carboxylation-limited above the T_{opt} at low leaf nitrogen content while, under high N level, it shifted to a limitation by RuBP regeneration. However, the effect of temperature on the limiting steps of A_n (V_{cmax} *vs.* J_{max}) may depend on the reponse of CO_2 conductance (g_s and g_m) as well (Benomar et al., 2018; Qiu et al., 2017; von Caemmerer and Evans, 2015; Warren, 2008). Moreover, RuBisCO-related effect on A_n at above-optimal temperature may depend on the plasticity of J_{max}^{25} to V_{cmax}^{25} ratio. From this perspective, this may be applicable only for cold-adapted plant species, which are characterized by a higher J_{max}^{25} to V_{cmax}^{25} ratio and low or lack of its adjustment in response to both N level and growth temperature (Benomar et al., 2018; Kattge and Knorr, 2007). Weston et al. (2007) did not observe any change in RuBisCO concentration for two genotypes of *Acer rubrum* grown under hot and optimal temperatures. Then, more research is needed to unravel the multiple

89 factors involved in the response of carbon assimilation to above-optimal temperatures. In
90 fact, it has been proven that V_{cmax} do not only depend on RuBisCO concentration but also
91 on its activation state (inhibited/activated) (Cen and Sage, 2005; Sage et al., 2008; Salvucci
92 and Crafts-Brandner, 2004). The activation state of RuBisCO is regulated by the RuBisCO
93 activase (*RCA*), a heat-labile enzyme using eneregy via ATP hydrolysis to release
94 inhibitors from the active site of RuBisCO (Crafts-Brandner and Salvucci, 2000; Salvucci
95 and Crafts-Brandner, 2004; Yamori and von Caemmerer, 2009). A decrease in *RCA*
96 activity has been documented as a primary cause of reducing RuBisCO activity and then
97 photosynthetic performance in response to increasing growth temperature (Hozain et al.,
98 2009; Salvucci and Crafts-Brandner, 2004; Yamori and von Caemmerer, 2009). *RCA* is a
99 stromal protein existing in two isoforms of 41–43 kDa (short isoform) and 45–46 kDa (long
100 isoform) that arises from one single gene with alternatively spliced transcript or from two
101 separate genes. Still, the specific physiological role of a given isoform with respect to heat
102 stress is generally not understood. Recent studies from herbaceous species demonstrated
103 an increase in the two *RCA* forms or a shift in the balance between them when plants were
104 exposed to temperature above 30°C (Law et al., 2001; Ristic et al., 2009; Wang et al., 2010;
105 Weston et al., 2007; Yamori et al., 2014).

106 Here we used *Populus* to study the physiological thermal acclimation because of its
107 commercial and environmental importance in the northern hemisphere and its fast growth
108 rate. Information on the response of photosynthesis to higher temperature for tree species
109 is limited in general, and previous studies conducted on *Populus balsamifera* (Silim et al.,
110 2010), *Populus tremuloides* (Dillaway and Kruger 2010), *Populus nigra* (Centritto et al.,
111 2011), *Populus grandidentata* (Gunderson et al., 2010) and *Populus deltoides* × *nigra*. (Ow

et al., 2008) found little evidence of a thermal acclimation of A_n to increasing temperatures. Nevertheless, little research focused on the physiological and molecular mechanisms underlying the observed thermal acclimation of trees. The objective of the present study was to examine to what extent leaf nitrogen, RuBisCO and RCA content are involved in thermal acclimation of photosynthetic activity in hybrid poplars.

Methodology

Plant material and growth conditions

This experiment was conducted in greenhouses and growth chambers at Université Laval, Québec, Canada, from January to May 2017. Dormant cuttings of two hybrid poplar clones: M×N (*Populus maximowiczii* × *Populus nigra*) and M×B (*Populus maximowiczii* × *Populus balsamifera*) were provided by the Québec's Ministère des Forêts, de la Faune et des Parcs from the forest nursery of Berthier (Berthierville, Québec, Canada) during early January after chilling needs were met. Cuttings were planted in 2 L pots filled with peat/vermiculite substrate (v/v=3/1) and placed in two greenhouses where day/night temperatures were 23°C/18°C and 33°C/27°C. Plants were grown under a photosynthetically active radiation (*PAR*) ranging between 400 and 700 µmol m^{-2} s^{-1}, a relative humidity of 65% and a 8/16 h dark/light photoperiod using 400 W metal halide lamps. Cuttings were irrigated daily to maintain full soil field capacity. After 4 weeks, for a better control of growth conditions (mainly temperature and relative humidity), pots were transferred to growth chambers (model PGW 36, Conviron, Winnipeg, Canada) under a split-split-plot layout; the Temperature×Clone as first split and Nitrogen level as second

split. The same environment parameters as in greenhouses were used, except PAR, which was kept at a constant rate of 500 µmol m^{-2} s^{-1} during day time. In each growth chamber, half of plants (n=18) were randomly assigned to receive a low-nitrogen fertilization treatment (5 mM) while the other half received a high-nitrogen (20 mM). Nitrogen was added, every week, using (20N-20P-20K) fertilizer dissolved in distilled water. Plants (n = 72; 2 growth temperatures × 2 nitrogen levels × 2 hybrid poplar clones × 9 replicates) were allowed to acclimate to respective growth conditions for 6 weeks before measurements were taken. Pots were moved within each chamber every third day to eliminate any position-related bias.

Gas exchange measurements

After 10 weeks of growth, leaf-level gas exchange were measured on the 4th fully expanded leaf from the top of each plant using two cross-calibrated portable open-path gas-exchange systems (Li-6400, Li-Cor Inc., Lincoln NE), equipped with a leaf chamber fluorometer (Li-6400-40, Li-Cor Inc). The measurements were made on 24 plants in total (3 replicates × 2 clones × 2 temperatures × 2 N levels). Given the limited control capacity of LI-6400 system on leaf temperature in the cuvette (T_{leaf} can be set to ± 6°C of the ambient temperature), measurements were performed in a growth chamber under controlled temperature and relative humidity. Growth chamber temperature was set manually to desired T_{leaf} allowing an effective and quick easy adjustment over the 10 - 40°C range and an exposure of the whole plant to the targeted temperature.

Temperature was increased from 10°C to 40°C with 5°C increment and plants were allowed to acclimate for at least 20 min to each step. At each temperature, we measured dark respiration (R_d) followed by A-C_i response curve records with 10-minutes period between R_d and A-C_i respected to allow complete opening of stomata. A-Ci response curves were recorded at each temperature after at least 10 min of steady state at ambient CO_2 partial pressure C_a=400 µmol mol^{-1} and a saturated photosynthetic active radiation PAR=800 µmol m^{-2} s^{-1}. The saturated PAR was determined from measured A-Q curve on 3 plants from each Clone×Growth T° combination at 25°C. Thereafter, the reference CO_2 (C_a) was changed in the following order: 400, 350, 300, 200, 100, 50, 400, 500, 600, 800, 900, 1000, 1200, 1400, and 1600 µmol mol^{-1}. Values were recorded based on the stability of photosynthesis, stomatal conductance (g_s), CO_2 and water vapor concentration. The vapor pressure difference (VPD) during measurement varied from 0.5 to 3.2 KPa from low to high temperature and was lowered as much as possible at high temperature by maintaining relative humidity (RH) at 70% inside the growth chamber. Similarly, RH was maintained at 50% to maintain VPD as high as 0.5 KPa at low temperature. The list of abbreviations and symbols are given in Table 1.

173 Table 1: List of abbreviations

174

Symbol	Definition	Unit
A_c	RuBP-saturated CO_2 assimilation rate	μmol CO_2 m^{-2} s^{-1}
A_{growth}	Photosynthetic rate at growth temperature	μmol CO_2 m^{-2} s^{-1}
A_n	Net CO_2 assimilation rate	μmol CO_2 m^{-2} s^{-1}
A_j	RuBP-limited CO_2 assimilation rate	μmol CO_2 m^{-2} s^{-1}
A_{opt}	Photosynthetic rate at T_{opt}	μmol CO_2 m^{-2} s^{-1}
C_a	Atmospheric CO_2 concentration	µmol mol^{-1}
C_i	intercellular CO_2 concentration	µmol mol^{-1}
E_a	Energy of deactivation	KJ mol^{-1}
E_d	Activation energy	KJ mol^{-1}
g_s	Stomatal conductance	mol H_2O m^{-2} s^{-1}
J	Electron transport rate	μmol m^{-2} s^{-1}
J_{max}^{25}	Maximal electron transport rate at leaf temperature of 25°C	μmol m^{-2} s^{-1}
$J_{max}^{25}:V_{cmax}^{25}$	Ratio of maximal electron transport to maximal carboxylation rate at leaf temperature of 25°C	
N_{area}	Leaf nitrogen in area basis	g m^{-2}
O	Partial atmospheric pressure of O_2	mmol mol^{-1}
PAR	Photosynthetically active radiation	μmol m^{-2} s^{-1}
SLA	Specific leaf area	cm^2 g^{-1}
R_{day}	Mitochondrial respiration in the light	μmol CO_2 m^{-2} s^{-1}
R_d	Dark respiration	μmol CO_2 m^{-2} s^{-1}
R_d^{10}	*Rd* at leaf temperature of 10°C	μmol CO_2 m^{-2} s^{-1}
RCA	RuBisCO activase	
T_{opt}	Thermal optimum	°C
K_c	Michaelis–Menten constants of Rubisco for CO_2	µmol mol^{-1}
K_o	Michaelis–Menten constants of Rubisco for O_2	mmol mol^{-1}
Q_{10}	Rate of change in R_d with a 10°C increase in temperature	
Γ^*	CO_2 compensation point in the absence of mitochondrial respiration	µmol mol^{-1}
α	Efficiency of light energy conversion	
V_{cmax}	Maximal carboxylation rate	μmol CO_2 m^{-2} s^{-1}
V_{cmax}^{25}	Maximal carboxylation rate at leaf temperature of 25°C	μmol CO_2 m^{-2} s^{-1}

175

176

177 **Estimation of gas exchange parameters**

178 The photosynthetic capacity variables ,V_{cmax} and J_{max}, were estimated from gas-exchange
179 by fitting the A-C_i curve with the biochemical model of C_3 (Farquhar et al., 1980), assuming
180 infinite mesophyll conductance (g_m). In fact, the estimation of g_m from A-Ci is very
181 challenging as it depends on the number of data points on the A-Ci curve and goodness -
182 of-fit of the curve which is difficult to achieve at high and low temperatures. In this
183 experiment, we tried to estimate g_m from A-Ci curves following Ethier et al. (2004) and
184 Miao et al. (2008) without success as about 45 % of them gave non-meaningful estimates.
185 The model was thus fitted using non-linear regression techniques (Proc NLIN, SAS)
186 following Dubois et al. (2007). Briefly, the net assimilation rate (A_n) is given as:

187 $$A_n = min\{A_c, A_j\} \quad \textbf{(1)}$$

188 $$A_c = V_{cmax}\frac{(C_i - \Gamma^*)}{C_i + K_c\left(1 + {}^{O}/_{K_o}\right)} - R_{day} \quad \textbf{(2)}$$

189 $$A_j = J\frac{C_i - \Gamma^*}{4(C_i + 2\Gamma^*)} - R_{day} \quad \textbf{(3)}$$

190 $$J = \frac{\alpha\, Q}{\sqrt{1 + (\frac{\alpha Q}{J_{max}})^2}} \quad \textbf{(4)}$$

191

192 where V_{cmax} is the apparent maximum rate of carboxylation (μmol CO_2 m^{-2} s^{-1}), O is the
193 partial atmospheric pressure of O_2 (mmol mol^{-1}), Γ^* is the CO_2 photo-compensation point
194 in the absence of mitochondrial respiration, R_{day}, is mitochondrial respiration in the light
195 (μmol CO_2 m^{-2} s^{-1}), C_i is the intercellular (substomatal) concentration of CO_2 (µmol mol^{-1}),
196 K_c (µmol mol^{-1}) and K_o (mmol mol^{-1}) are the Michaelis–Menten constants of Rubisco
197 for CO_2 and O_2, respectively, J is the apparent rate of electron transport (μmol CO_2 m^{-2} s^{-}

198 ^{1}), J_{max} is the apparent maximum rate of electron transport (μmol CO_2 m^{-2} s^{-1}), Q is the
199 incident PAR (μmol m^{-2} s^{-1}), α is the efficiency of light energy conversion (0.18) which
200 represents the initial slope of the photosynthetic light response curve (Miao et al., 2008).
201 The values at 25°C used for K_c, K_o and Γ^* were 272 µmol mol^{-1}, 166 mmol mol^{-1} and 37.4
202 µmol mol^{-1}, respectively (Sharkey et al., 2007) and their temperature dependency were as
203 in Sharkey et al.(2007. Most of A-C_i curves at 35°C and 40 °C measured for low nitrogen
204 level at 23 °C failed to converge and estimates of V_{cmax} and J could not be obtained.

205 **Characterization of the temperature responses of gas exchange parameters**

206 Photosynthesis temperature response curves were fitted individually with a quadratic
207 model following Battaglia et al. (1996):

208 $$A_n(T) = A_{opt} - b(T - T_{opt})^2 \quad \textbf{(5)}$$

209 where $A_n(T)$ is the photosynthetic rate at temperature T in °C, A_{opt} is the photosynthetic rate
210 at the temperature optimum (T_{opt}) and the parameter b describes the spread of the parabola.
211 A_{growth} was then estimated using the obtained parameters from equation (5) for each
212 individual curve. Daytime temperature was used as growth temperature given the
213 uncertainty regarding the effect of nighttime temperature on A_n.

214

215 Dark respiration temperature response curves were fitted with a model in equation (6) to
216 estimate the Q_{10} (the change in respiration with a 10°C increase in temperature) following
217 Atkin et al. (2005):

218 $$R_d(T) = R_d{}^{10} Q_{10}{}^{[(T-10)/10]} \quad \textbf{(6)}$$

219 where $R_d{}^{10}$ is the measured basal rate of R_d at the reference temperature of 10°C.

220

221 The responses of V_{cmax} and J to leaf temperature were fitted using the following two models
222 (equation (7) and (8)) depending on the presence or not of deactivation above thermal
223 optimum following Medlyn et al. (2002):

224 $$f(T_k) = e^{\left(c - \frac{E_a}{RT}\right)} \quad \textbf{(7)}$$

225 $$f(T_k) = k_{opt} \frac{E_d \, exp^{\left[\frac{E_a(T_k - T_{opt})}{T_k R T_{opt}}\right]}}{E_d - E_a\left[1 - exp^{\left(\frac{E_d(T_k - T_{opt})}{T_k R T_{opt}}\right)}\right]} \quad \textbf{(8)}$$

226 where E_a is the activation energy, E_d is the energy of deactivation, K_{opt} is the V_{cmax} or J at
227 the temperature optimum (T_{opt}). E_d was fixed at 200 KJ mol^{-1} (Medlyn et al., 2002) to
228 reduce the number of estimated parameters to three.

229

230 **SLA and leaf nitrogen**

231 Leaves used for gas exchange measurements were collected and immediately placed in dry
232 ice before being stored at -20°C and processed within a week for protein extraction. The
233 extracts were conserved under -80°C and dosage of proteins (RuBisCO and RCA) was
234 done once all samples were extracted. Symmetric leaves (by the stem) were also collected
235 to measure projected area with WinSeedle (Version 2007 Pro, Regent Instruments, Québec,
236 Canada). Samples were then oven-dried for 72h at 56 °C, and their dry mass determined.
237 Specific leaf area (*SLA*) was calculated as the ratio of the projected leaf area (cm^2) to the
238 leaf dry mass (g). Later, leaves were ground separately and N content determined at

239 Université Laval using a LECO elemental analyser (LECO Corporation, St Joseph, MI,
240 USA).

241 **Extraction and dosage of RuBisCO and RuBisCO activase**

242 Proteins were extracted from frozen leaves at -20 °C within less than one week after leaf
243 harvesting following the method outlined in Yamori and von Caemmerer (2009). Briefly,
244 100 mg of leaves were initially ground in liquid nitrogen using a mortar and pestle. Proteins
245 were extracted on ice using a protein extraction buffer containing 50 mM Hepes-KOH pH
246 7.8, 10 mM $MgCl_2$, 1 mM EDTA, 5 mM DTT, 0.1% triton X100 (v/v) and protease
247 inhibitor cocktail (Roche). The extracts were conserved under -80°C. Once all samples
248 were extracted, the solutions were centrifuged at 16,000g for 1 min followed by
249 determination of the concentration of total soluble proteins (TSP) in supernatant by the
250 Bradford method (Bradford, 1976).
251 After dosage, 4× sample buffer (250 mM Tris–HCl, pH 6.8, 40% glycerol, 8% SDS, 0.2%
252 Bromophenol-blue, 200 mM DTT) was added to proteins extracts, heated at 100 °C for 5
253 min and then centrifuged at 16,000 g for 5 min. After cooling to room temperature, a
254 volume representing 20 µg of total TSP extract of each sample was loaded onto 12% SDS-
255 polyacrylamide gel electrophoresis (SDS-PAGE). The electrophoresis was carried out at
256 room temperature at a constant voltage (120 V). Following SDS-Page, the proteins were
257 transferred to a nitrocellulose membrane (Life Sciences, Mississauga, Canada) for western
258 blot.
259 Blots were incubated with 5% non-fat milk in TBST (50 mM Tris, pH 7.5, 150 mM NaCl,
260 0.1% Tween-20) for 60 min, the membranes were washed twice with TBST and incubated
261 with antibodies against RuBisCO (Agrisera AB, Vännäs, Sweden) or against RuBisCO

activase (Agrisera AB, Vännäs, Sweden) at room temperature for 60 min. Membranes were washed three times with TBST for 10 min and incubated with secondary antibodies peroxidase-conjugated (Goat Anti-Chicken (abcam) for RuBisCO and Goat Anti-Rabbit (abcam) for RuBisCO activase) during 60 min at room temperature. Blots were washed with TBST three times and developed with the ECL system using Odyssey® Infrared Imaging System (Li-COR, Biosciences). Images were analysed using ImageJ (Rasband, 2016) to determine band densities of each sample. The RuBisCo, *RCA* and its two isoforms concentration were expressed as relative to the sample representing the highest density (Perdomo et al., 2017; Prins et al., 2008; Ristic et al., 2009).

Statistical analysis

Three-way analysis of variance was performed to test the effect of growth temperature, clone and nitrogen level on response variables using MIXED procedure of SAS (SAS Institute, software version 9.4, Cary, NC, USA). We used proc Glimmix for response variables (apparent V_{cmax}^{25}, apparent J_{max}^{25} and E_a) which did not met the assumptions of residual normality and homoscedasticity even with transformations. Means were compared by the adjusted Tukey method and differences were considered significant if $P \leq 0.05$.

Results

Temperature response of A_n and R_d

The temperature response curve of net photosynthesis at saturated light (A_n) followed a common parabolic shape (Fig. 1a, 1b). The two hybrid poplar clones adjusted their thermal

284 optimum (T_{opt}) of A_n in response to growth temperature. Low nitrogen level constrained the
285 adjustment of T_{opt} for clone M×N but not M×B (Table 2). Also, T_{opt} was lower than growth
286 temperature except for clone M×B at 23°C. The two hybrid poplar clones showed different
287 trends regarding A_n at T_{opt} (A_{opt}) which increased with increasing growth temperature for
288 clone M×B and remained unaffected for clone M×N. A_{growth} had a similar trend as A_{opt} in
289 response to growth temperature and N level. Both A_{growth} and A_{opt} declined at low N level
290 for both clones (Table 2).

291 The two hybrid poplar clones had different strategies in term of thermal response of dark
292 respiration (R_d) (Fig. 1c, 1d). Irrespective of N level, basal rate of R_d (R_d^{10}) decreased by
293 augmenting growth temperature for clone M×B but remained unchanged for clone M×N
294 (Table 2). The rate of change in R_d by 10°C change in temperature, Q_{10}, decreased when
295 growth temperature was increased, irrespective of N level for clone M×N. In contrast, Q_{10}
296 of clone M×B increased in response to growth temperature raise when N level was high
297 and unchanged at low N level (Table 2).

298

299 **Fig 1.** Response of net photosynthesis (A_n) and dark respiration (R_d) to leaf temperature for
300 hybrid poplar clone M×B (a, c) and clone M×N (b, d) grown under two temperatures and
301 two nitrogen levels.

302 H23 and L23 are treatments of high and low nitrogen level respectively at an ambient day
303 temperature of 23°C; H33 and L33 are treatments of high and low nitrogen level at 33°C
304 ambient day temperature. Data are represented by means ± SE (n=3). P value and R^2 of
305 curves are given in Table S1.

306

307

Table 2: Means (±SE) of thermal acclimation-related traits of two hybrid poplar clones (M×B and M×N) grown at day/night temperature of 23/18°C and 33/27°C under high (HN) and low (LN) nitrogen levels (n=3).

	Clone M×B				**Clone M×N**			
	23°C		**33°C**		**23°C**		**33°C**	
	HN	**LN**	**HN**	**LN**	**HN**	**LN**	**HN**	**LN**
$T_{opt}(A_n)$	23.1 (1.2)^{bc}	24.1 (1.2)b	30.3 (1.3)a	29.3 (1.3)a	20.5 (1.2)c	19.7 (1.3)c	30.1 (1.3)a	26.1 (1.3)b
A_{opt}	10.1 (0.8)b	7.1(0.8)d	14.9 (0.8)a	9.3 (0.8)cb	15.1 (0.8)a	9.1 (0.8)c	14.2 (0.8)a	10.9 (0.8)b
A_{growth}	10.6(1.0)b	6.9(0.9)c	13.9(1.1)a	8.9(1.1)c	14.9(1.1)a	9.6(0.9)c	13.4(1.1)a	9.5(1.1)c
Rd_{10}	0.76(0.1)b	0.80(0.1)ab	0.60(0.1)cd	0.70(0.1)c	0.90(0.1)a	0.56(0.1)d	0.90(0.1)a	0.71(0.2)cd
Q_{10} (Rd)	1.9(0.1)b	1.8(0.1)b	2.0(0.1)a	1.9(0.1)b	2.0(0.1)a	2.2(0.1)a	1.8(0.1)b	1.8(0.1)b
g_{s_growth}	0.16(0.01)c	0.17(0.01)bc	0.26(0.01)a	0.20(0.01)b	0.20(0.01)b	0.16(0.01)c	0.18(0.01)cb	0.13(0.01)d
V_{cmax}^{25}	53(6)c	34(6)d	70(6)ab	38(6)d	78(6)a	54(6)bc	62(7)b	53(6)bc
J_{max}^{25}	146(7)b	67(7)d	106(6)c	74(9)d	240(9)a	124(7)c	162(8)b	107(8)c
$T_{opt}(V_{cmax})$	33(1.5)	-	NA	NA	34(1.2)	-	NA	NA
$E_a(V_{cmax})$	75 (3)a	-	49(3)b	57(3)b	58(3)b	-	54(3)b	55(3)b
$T_{opt}(J)$	34 (1.9)	-	NA	NA	30(1.1)	-	NA	NA
$E_a(J)$	46(2)a	-	32(2)b	28(2)b	34(2)ab	-	28(2)b	33(2)b
$J_{max}^{25}:V_{cmax}^{25}$	2.43(0.1)ab	1.68(0.15)c	1.53(0.15)c	1.81(0.19)bc	2.68(0.15)a	2.01 (0.15)bc	2.42(0.19)ab	1.95(0.16)b
SLA	172(7)a	132(7)cd	154(8)b	123(7)d	143(7)b	141(7)bc	136(8)c	112(8)e
N_{area}	1.3(0.1)b	0.8(0.1)d	1.3(0.1b)	0.8(0.1)d	1.9(0.1)a	1.1(0.1)c	1.4(0.1)b	1.1(0.1)c

Within rows, means followed by the same letter do not differ significantly at α=0.05 based on Tukey's test

311 **Temperature response of apparent V_{cmax} and J**

312 Apparent V_{cmax}^{25} was insensitive to growth temperature at low N level for both clones. In
313 contrast, at high N level, apparent V_{cmax}^{25} increased for clone M×B and decreased for clone
314 M×N when growth temperature was increased (Table 2). Apparent J_{max}^{25} decreased with
315 increasing growth temperature for plants growing at high N level and was insensitive to
316 growth temperature at low N level. The ratio J_{max}^{25}: V_{cmax}^{25} decreased with increasing
317 growth temperature at high N level for clone M×B but not for clone M×N (Table 2). At
318 low N level, J_{max}^{25}:V_{cmax}^{25} ratio was insensitive to growth temperature.

319 The temperature response curve of apparent V_{cmax} and apparent J were affected by growth
320 temperature but not by nitrogen level. In fact, at cooler growth temperature, apparent V_{cmax}
321 peaked at 33°C and 34°C (Fig. 2; Table 2) and apparent J peaked at 34°C and 30°C (Fig.
322 2; Table 2) for clones M×B and M×N respectively. However, apparent V_{cmax} and apparent
323 J did not show any deactivation at warm temperature (Fig. 2). The activation energy (E_a)
324 of apparent V_{cmax} and J, decreased with increasing growth temperature for clone M×B and
325 remained constant for clone M×N (Table 2).

326 **Fig 2.** The temperature dependence of the apparent maximum carboxylation capacity of
327 RuBisCO (V_{cmax}) and the apparent electron transport rate (J) for clone M×B (a, c) and clone
328 M×N (b, d) grown under two temperatures and two nitrogen levels.

329 See Fig 1 for symbols. L23 treatment was not given for both clones because A-Ci curves
330 at 35 and 40 °C failed to converge and estimates of V_{cmax} and J could not be obtained. Data
331 are represented by means ± SE (n=3). P value and R^2 of curves are given in Table S1

332

333

334

335 **Temperature response of stomatal conductance (g_s)**

336 g_s decreased under all treatments and for both clones when T_{leaf} was increased over the 10-
337 40°C gradient (Fig. 3). g_s at the growth temperature, derived from the g_s-T response curves
338 (g_{s_growth}) was influenced by both clone and growth temperature. For clone M×B, g_{s_growth}
339 was 62.5 % and 17 % higher at warm, compared to cooler growth temperature under high
340 and low nitrogen level respectively (Table 2). Conversely, for clone M×N, g_{s_growth} was
341 similar among growth temperature at high N level averaging 0.19 mol H_2O m^{-2} s^{-1} and
342 decreased by increasing growth temperature at low N level (0.16 vs. 0.13 mol H_2O m^{-2}
343 s^{-1}).

344

345 **Fig 3.** Response of stomatal conductance (g_s) to leaf temperature of two hybrid poplar
346 clones (M×B) and (M×N) grown under two temperatures and two nitrogen levels (n=3).
347 See Figure 1 for symbols. Data are represented by means ± SE (n=3). P value and R^2 of
348 curves are given in Table S1

349

350

351 **RuBisCO and RuBisCO activase amount**

352 Relative amount of RuBisCO (*RAR*) decreased significantly when N level changed from
353 high to low (Fig. 4a). *RAR* did not change in response to change of growth temperature for
354 both clones (Fig. 4a). In addition, at high N level, *RAR* was similar between clones, being
355 around 0.8 on average. At low N level, RAR was two folds higher for clone M×N compared

356 to clone M×B (Fig. 4a). Nitrogen enrichment remarkably increased the relative amount of
357 RuBisCO activase (*RARCA*), particularly for clone M×N which had a lower *RARCA* at low
358 N level, compared to M×B (Fig. 4b). Except for clone M×B at high N, *RARCA* was
359 stimulated by warmer growth temperature (Fig. 4b). More importantly, the ratio of short
360 isoform to large isoform of *RCA* was markedly simulated by warm conditions for clone
361 M×N and only at low N for clone M×B (Fig. 5).

362

363 **Figure 4**: Relative amounts of RuBisCO (a) and RuBisCO-activase (b) measured by
364 western blot for two hybrid poplar clones (M×B) and (M×N) grown under two
365 temperatures and two nitrogen levels (n=3).

366 Proteins were extracted from leaves and analysed by SDS-PAGE. Immunoblots were
367 probed with anti-Rubisco or anti-RCA antibody. H23 and L23 are treatments of high and
368 low nitrogen level respectively at 23°C ambient daytime temperature; H33 and L33 are
369 treatments of low and high nitrogen level at 33°C ambient daytime temperature. Data are
370 represented by means ± SD (n=3). Means having the same letters are not significantly
371 different at $\alpha = 0.05$ based on Tukey's tests.

372

373 **Figure 5**: Ratio of short to long isoform of RuBisCO-activase (RCA) of two hybrid poplar
374 grown under two temperatures and two nitrogen levels (n=3).

375 RCA-S: short isoform of RCA; RCA-L: long isoform of RCA. Data are represented by
376 means ± SE (n=3). Means having the same letters are not significantly different at $\alpha = 0.05$
377 based on Tukey's tests.

378

379

DISCUSSION

Thermal acclimation of A_n and R_d

The two hybrid poplar clones showed a clear thermal acclimation of A_n by adjusting A_{opt} and/or T_{opt} to growth tempearture. This is in accordance with results of Silim et al. (2010) on cold and warm ecotypes of *Populus balsamifera* which maintained A_{opt} without an evident change of T_{opt}. We found that T_{opt} of A_n under warm tempearture was identical to mean growth temperature (the average of day time/night-time =30°C) and was 3°C below the daytime growth temperature (33°C) suggesting a partial acclimation of photosynthesis rate if we assume the latter was unrelated to night-time temperature. So far, studies focusing on night-time temperature effect on A_n are very scarce (Turnbull et al., 2002). T_{op} of A_n for clone M×N was lowered by low nitrogen level under warms conditions. This result is difficult to explain from traits measured in our study and could be an outcome of a differential expression of proteins. The net photosynthetic rates at the growth temperature (A_{growth}), a relevant quantitative trait of thermal acclimation of A_n (Way and Yamori, 2014; Yamori et al., 2014), was enhanced in plants grown at the warm temperature for clone M×B and remained unchanged for clone M×N. These results suggest a differential thermal adaptation range of the two hybrid poplar clones which could result from the climate of origin of their parents. Hence, the choice of suitable clones based on their thermal acclimation capacity would increase productivity of hybrid poplar plantations under future warming conditions, particularly in heat-prone regions like the south of Québec, Canada.

Thermal acclimation of R_d is very common for C_3 plants and several studies reported a downshift of R_d^{10} (Type II acclimation) and a decrease of Q_{10} (Type I acclimation) in

403 reponse to warmer temperatures (Atkin and Tjoelker, 2003; Reich et al., 2016) but few
404 studies on *Populus* exist in this regard (Dillaway and Kruger, 2011; Ow et al., 2008; Silim
405 et al., 2010; Tjoelker et al., 1999). In accordance with the finding of Tjoelker et al. (1999)
406 for *Populus tremula* , we found substantial Type I acclimation of R_d (downshift of Q_{10}) to
407 growth temperature for clone M×N. In contrast, no acclimation of R_d was observed for
408 clone M×B which may be related to the unchanged density of mitochondria (Atkin and
409 Tjoelker, 2003). Moreover, nitrogen had no effect on thermal acclimation of Q_{10} for both
410 clones as observed in other tree species (Benomar et al., 2018; Tjoelker et al., 1999).
411
412 **Thermal response of photosynthetic biochemical limitations**
413 The effect of growth temperature on temperature response curve of apparent V_{cmax} and J in
414 terms of their values at reference temperature of 25°C, their T_{opt} and their activation energy
415 is species-dependant as reported by recent studies (Benomar et al., 2018; Hikosaka et al.,
416 2006; Hikosaka et al., 1999; Kattge and Knorr, 2007; Slot and Winter 2017; Way and
417 Yamori 2014). In our study, the apparent V_{cmax}^{25} stimulated by warm growth temperature
418 for clone M×B, might explain the noticeable increase of A_{opt} (up to 50 %) by warmer
419 growth conditions under high N level. In parallel, the small decrease in the apparent V_{cmax}^{25}
420 at warm growth conditions observed for clone M×N might explain the observed similar
421 A_{opt} under the two growth temperature. These results are in agreement with the findings of
422 other studies showing a similar or a greater V_{cmax}^{25} when growth temperature increased
423 (Aspinwall et al., 2017; Silim et al., 2010; Way and Yamori, 2014; Slot and Winter, 2017).
424 In contrast, the apparent J_{max}^{25} decreased at warmer growth temperature as reported for

425 *Populus balsamifera* (Silim et al., 2010) and other tree species (Yamori et al., 2008; Way
426 and Yamori, 2014; Slot and Winter, 2017).
427 Hikosaka et al. (2006) suggested the increase in the activation energy of V_{cmax} (Ea) with the
428 increase in growth temperature as an explanatory mechanism of thermal acclimation of A_n
429 (at least by the increase of T_{opt} with growth temperature). Our results are diverging with
430 this postulate since we obseved no change in E_a for clone M×N and a remarkable decrease
431 of E_a for clone M×B. However, the patterns we observed have been reported for several
432 species including *Populus tremuloides* (Dillaway and Kruger, 2010), *Populus balsamifera*
433 (Silim et al., 2010) and *Corymbia calophylla* (Aspinwall et al., 2017).
434 The temperature optimum (T_{opt}) of apparent V_{cmax} and J acclimated to growth temperature
435 (Fig. 2) as observed for others species (Kattge and Knorr, 2007; Crous et al., 2018) and
436 may have contributed in the observed acclimation of A_n (Fig. 1). Under cooler conditions,
437 T_{opt} of apparent V_{cmax} and J were similar but much higher than that of A_n indicating a very
438 likely involvement of other traits in the observed value of T_{opt} of A_n under this condition
439 (23 °C).
440
441 The adjustment of leaf nitrogen invested in soluble *vs*. insoluble proteins in response to
442 change in growth temperature, inferred from J_{max}^{25} to V_{cmax}^{25} ratio, can be achieved through
443 the maintenance of an optimal balance between the rate of photosynthetic carboxylation
444 *vs*. RuBP regeneration.This mechanism allows plants to maximize the photosynthetic rate
445 at a given growth temperature (Hikosaka et al., 1999; Kattge and Knorr, 2007). Therefore,
446 the decrease of J_{max}^{25}:V_{cmax}^{25} ratio consequent to an increase of growth temperature has
447 been reported to significantly contribute to thermal acclimation of A_n (Kattge and Knorr,

448 2007; Slot and Winter 2017; Crous et al., 2018). In our study, this pattern occurred for
449 clone M×B under high N level which has resulted in an increase of both V_{cmax}^{25} and A_{opt}.
450 Conversely, the lack of modulation of J_{max}^{25}:V_{cmax}^{25} ratio for clone M×N may have
451 contributed to the observed decrease in V_{cmax}^{25} and to the maintenance of A_{opt}. Under low
452 N level, A_{opt} of M×B increased under warmer conditions without any change of the
453 J_{max}^{25}:V_{cmax}^{25} ratio . Therefore, the increase of V_{cmax}^{25} and A_{opt} under the warm growth
454 temperature cannot be attributed only to the shift in J_{max}^{25}:V_{cmax}^{25} ratio.

455

456 **RuBisCO and RuBisCO activase amounts in response to experimental warming**

457 The RuBisCO content in our study was quite sensitive to nitrogen level but not to growth
458 temperature . Neither thermal acclimation of A_n (T_{opt} and A_{opt}) nor J_{max}^{25}:V_{cmax}^{25} ratio was
459 affected by RuBisCO content. The absence of any effect of RubisCO content on traits
460 related to thermal acclimation of A_n has been reported by Weston et al. (2007) and Kruse
461 et al. (2017), while other studies found a significant decrease of V_{cmax}^{25} linked to a decrease
462 in RuBisCO and leaf nitrogen content (Scafaro et al., 2016; Crous et al., 2018). Thus, the
463 relationship between the change in RuBisCO content in response to growth temperature
464 and thermal acclimation of A_n via the modulation of photosynthetic capacity attributes
465 (V_{cmax}^{25} and J_{max}^{25}) is, most likely, depending on species and environemental parameters
466 (e.g. nitrogen availibility). Indeed, CO_2 conductance, the variation of *RCA* content and the
467 temperature dependency of Rubisco kinetic properties have been rerported to be
468 determinant factors of the V_{cmax}^{25} response to growth temperature and consequently thermal
469 acclimation of A_n (Perdomoetal et al., 2017; Way and Yamori, 2014;Yamori et al., 2006;
470 Qiu et al., 2017). The increase of leaf *RCA* amount by increased growth temperature has

471 been reported for several tree species (Crafts-Brandner and Salvucci, 2000; Hozain et al.,
472 2009; Law et al., 2001; Ristic et al., 2009; Weston et al., 2007; Yamori and von Caemmerer,
473 2009). In our study, the hypothesized increase of *RCA* at warmer growth temperature was
474 observed, except for clone M×B at high N. More importantly, our results demonstrated that
475 the increase of the amount of *RCA* under warm conditions resulted mainly from increased
476 synthesis of the short isoform which indicates that the two isoforms operate at different
477 temperature optima.
478
479 **Stomatal conductance**
480 The contribution of diffusional limitations to thermal acclimation of A_n remain non-well
481 quantified for several species, including *Populus*. Our results demonstrate that the
482 modulation of g_s (the shape of the relationship between g_s and T_{leaf} and the value of g_s at
483 growth temperature) in response to change in growth temperature contributed to the
484 observed thermal acclimation of A_n (Figure 3) as observed by Aspinwall et al. (2017), Silim
485 et al. (2010) and Slot and Winter (2017). Also, our results suggest that the stomatal
486 acclimation to growth temperature may be clone-specific and may have a significant impact
487 on clone response to warming depending on soil water status. The CO_2 diffusion in the
488 mesophyll shares the same pathways of water transport from mesophyll to the atmosphere
489 (Ethier et al., 2004; Flexas et al., 2013) and may lead to similar response of stomatal and
490 mesophyll conductance to growth conditions. Moreover, a link between mesophyll
491 conductance (g_m) and hydraulic conductance has been reported as well (Flexas et al., 2013;
492 Théroux-Rancourt et al., 2014), suggesting that the observed response of g_s to growth
493 temperature may have originated from a modulation of g_m and hydraulic functioning.

494 In conclusion, the observed thermal acclimation of photosynthesis under our experimental
495 conditions was clearly related to the modulation of photosynthetic capacity and g_s in
496 response to growth temperature. The modulation of the photosynthetic capacity was mainly
497 linked to *RCA* but not RuBisCO content. Further investigation regarding the involvement
498 of mesophyll conductance and hydraulic conductivity should clarify the mechanistic basis
499 of the observed trends.

500 **Acknowledgements**

501 We thank Dr. G Ethier for his valuable comments on A-Ci curve analysis. We also thank
502 F Larochelle and M Coyea (Université Laval) for their technical assistance throughout the
503 project.

504 **References**

505 Aspinwall MJ, Vårhammar A, Blackman CJ, Tjoelker MG, Ahrens C, Byrne M, Tissue DT
506 and Rymer PD (2017) Adaptation and acclimation both influence photosynthetic
507 and respiratory temperature responses in *Corymbia calophylla*. Tree Physiol
508 37:1095-1112.
509 Atkin OK, Bruhn D and Tjoelker MG (2005) Response of plant respiration to changes in
510 temperature: Mechanisms and consequences of variations in Q_{10} values and
511 acclimation In: Lambers H, Ribas-Carbo M. eds. *Plant respiration: from cell to*
512 *ecosystem*. Dordrecht: Springer Netherlands.
513 Atkin OK and Tjoelker MG (2003) Thermal acclimation and the dynamic response of plant
514 respiration to temperature. *Trends in Plant Science* **8**:343-351.
515 Battaglia M, Beadle C and Loughhead S (1996) Photosynthetic temperature responses of
516 Eucalyptus globulus and Eucalyptus nitens. *Tree Physiol* **16**:81-89.
517 Benomar L, Lamhamedi MS, Pepin S, Rainville A, Lambert M-C, Margolis HA, Bousquet
518 J and Beaulieu J (2018) Thermal acclimation of photosynthesis and respiration of
519 southern and northern white spruce seed sources tested along a regional climatic
520 gradient indicates limited potential to cope with temperature warming. *Ann Bot*:.in
521 press.
522 Bradford MM (1976) A rapid and sensitive method for the quantitation of microgram
523 quantities of protein utilizing the principle of protein-dye binding. *Anal Biochem*
524 **72**:248-254.
525 Cen Y-P and Sage RF (2005) The regulation of rubisco activity in response to variation in
526 temperature and atmospheric CO_2 partial pressure in sweet potato. *Plant Physiol*
527 **139**:979-990.

528 Centritto M, Brilli F, Fodale R and Loreto F (2011) Different sensitivity of isoprene
529 emission, respiration and photosynthesis to high growth temperature coupled with
530 drought stress in black poplar (Populus nigra) saplings. *Tree Physiol* 31:275-286.
531 Crafts-Brandner SJ and Salvucci ME (2000) Rubisco activase constrains the
532 photosynthetic potential of leaves at high temperature and CO_2. *Proc Natl Acad Sci*
533 *USA* **97**:13430-13435.
534 DesRochers A, Van Den Driessche R and Thomas BR (2003) Nitrogen fertilization of
535 trembling aspen seedlings grown on soils of different pH. *Can J For Res* **33**:552-
536 560.
537 Dillaway DN and Kruger EL (2010) Thermal acclimation of photosynthesis: a comparison
538 of boreal and temperate tree species along a latitudinal transect. *Plant Cell Enviro*
539 **33**:888-899.
540 Dillaway DN and Kruger EL (2011) Leaf respiratory acclimation to climate: comparisons
541 among boreal and temperate tree species along a latitudinal transect. *Tree Physiol*
542 **31**:1114-1127.
543 Dubois JB, Fiscus EL, Booker F L, Flowers MD, and Reid CD (2007) Optimizing the
544 statistical estimation of the parameters of the Farquhar–von Caemmerer–Berry
545 model of photosynthesis. *New Phytol*, **176**: 402-414.
546 Ethier GJ and Livingston NJ (2004) On the need to incorporate sensitivity to CO_2 transfer
547 conductance into the Farquhar–von Caemmerer–Berry leaf photosynthesis model.
548 *Plant Cell Enviro* **27**:137-153.
549 Farquhar GD, von Caemmerer S and Berry JA (1980) A biochemical model of
550 photosynthetic CO_2 assimilation in leaves of C_3 species. *Planta.* **149**:78-90.
551 Field C (1983) Allocating leaf nitrogen for the maximization of carbon gain: Leaf age as a
552 control on the allocation program. *Oecol* **56**:341-347.
553 Fisichelli NA, Stefanski A, Frelich LE and Reich PB (2015) Temperature and leaf nitrogen
554 affect performance of plant species at range overlap. *Ecosphere.* **6**:1-4.
555 Flexas J, Scoffoni C, Gago J and Sack L (2013) Leaf mesophyll conductance and leaf
556 hydraulic conductance: an introduction to their measurement and coordination. *J*
557 *Exp Bot* 64:3965-3981.
558 Gunderson CA, O'Hara KH, Campion CM, Walker AV, Edwards NT (2010) Thermal
559 plasticity of photosynthesis: the role of acclimation in forest responses to a warming
560 climate. *Glob Chang Biol* **16**: 2272–2286.
561 Hikosaka K, Ishikawa K, Borjigidai A, Muller O and Onoda Y (2006) Temperature
562 acclimation of photosynthesis: mechanisms involved in the changes in temperature
563 dependence of photosynthetic rate. *J Exp Bot* **57**:291-302.
564 Hikosaka K, Murakami A and Hirose T (1999) Balancing carboxylation and regeneration
565 of ribulose-1,5-bisphosphate in leaf photosynthesis: temperature acclimation of an
566 evergreen tree, Quercus myrsinaefolia. *Plant Cell Enviro* **22**:841-849.
567 Hozain MdI, Salvucci ME, Fokar M and Holaday AS (2009) The differential response of
568 photosynthesis to high temperature for a boreal and temperate *Populus* species
569 relates to differences in Rubisco activation and Rubisco activase properties. *Tree*
570 *Physiol* **30**:32-44.
571 Kattge J and Knorr W (2007) Temperature acclimation in a biochemical model of
572 photosynthesis: a reanalysis of data from 36 species. *Plant Cell Environ* **30**:1176-
573 1190.

574 Kruse J, Adams MA, Kadinov G, Arab L, Kreuzwieser J, Alfarraj S, Schulze W and
575 Rennenberg H (2017) Characterization of photosynthetic acclimation in *Phoenix*
576 *dactylifera* by a modified Arrhenius equation originally developed for leaf
577 respiration. Trees **31**:623-644.
578 Law DR, Crafts-Brandner SJ and Salvucci ME (2001) Heat stress induces the synthesis of
579 a new form of ribulose-1,5-bisphosphate carboxylase/oxygenase activase in cotton
580 leaves. *Planta* **214**:117-125.
581 Lloyd J, Farquhar GD (2008) Effects of rising temperatures and CO2 on the physiology of
582 tropical forest trees. Philosophical Transactions of the Royal Society B: Biol
583 Sci**363**:1811-1817.
584 Medlyn BE, Dreyer E, Ellsworth D, Forstreuter M, Harley PC, Kirschbaum MUF, Le Roux
585 X, Montpied P, Strassemeyer J, Walcroft A, Wang K and Loustau D (2002)
586 Temperature response of parameters of a biochemically based model of
587 photosynthesis. II. A review of experimental data. *Plant Cell Environ* **25**:1167-
588 1179.
589 Miao Z, Xu M Lathrop RG and Wang Y (008) Comparison of the A–Cc curve fitting
590 methods in determining maximum ribulose 1·5-bisphosphate
591 carboxylase/oxygenase carboxylation rate, potential light saturated electron
592 transport rate and leaf dark respiration. Plant Cell Environ 32:109-122
593 Ow LF, Griffin KL, Whitehead D, Walcroft AS and Turnbull MH (2008) Thermal
594 acclimation of leaf respiration but not photosynthesis in Populus deltoides x nigra.
595 New Phytol 178:123-134.
596 Perdomo JA, Capó-Bauçà S, Carmo-Silva E and Galmés J (2017) Rubisco and Rubisco
597 Activase Play an Important Role in the Biochemical Limitations of Photosynthesis
598 in Rice, Wheat, and Maize under High Temperature and Water Deficit. Frontiers in
599 Plant Science 8.
600 Prins A, van Heerden PDR, Olmos E, Kunert KJ and Foyer CH (2008) Cysteine proteinases
601 regulate chloroplast protein content and composition in tobacco leaves: a model for
602 dynamic interactions with ribulose-1,5-bisphosphate carboxylase/oxygenase
603 (Rubisco) vesicular bodies. *J Exp Bot* **59**:1935-1950.
604 Poorter H, Niinemets Ü, Poorter L, Wright IJ and Villar R (2009) Causes and consequences
605 of variation in leaf mass per area (LMA): a meta-analysis. *New Phytol* **182**:565-
606 588.
607 Qiu C, Ethier G, Pepin S, Dubé P, Desjardins Y and Gosselin A (2017) Persistent negative
608 temperature response of mesophyll conductance in red raspberry (Rubus idaeus L.)
609 leaves under both high and low vapour pressure deficits: a role for abscisic acid?
610 *Plant Cell Environ* **40**:1940-1959.
611 Rasband WS (2016) ImageJ, U. S. National Institutes of Health, Bethesda, Maryland, USA.
612 Reich PB and Oleksyn J (2004) Global patterns of plant leaf N and P in relation to
613 temperature and latitude. *Proc. Natl. Acad. Sci USA* **101**:11001-11006.
614 Reich PB, Sendall KM, Stefanski A, Wei XR, Rich RL and Montgomery RA (2016) Boreal
615 and temperate trees show strong acclimation of respiration to warming. *Nature*
616 **531**:633-636.
617 Ristic Z, Momčilović I, Bukovnik U, Prasad PVV, Fu J, DeRidder BP, Elthon TE and
618 Mladenov N (2009) Rubisco activase and wheat productivity under heat-stress
619 conditions. *J Exp Bot* **60**:4003-4014.

620 Sage RF and Kubien DS (2007) The temperature response of C3 and C4 photosynthesis.
621 *Plant Cell Environ* **30**:1086-1106.
622 Sage RF, Way DA and Kubien DS (2008) Rubisco, Rubisco activase, and global climate
623 change. *J Exp Bot* **59**:1581-1595.
624 Salvucci ME and Crafts-Brandner SJ (2004) Relationship between the Heat Tolerance of
625 Photosynthesis and the Thermal Stability of Rubisco Activase in Plants from
626 Contrasting Thermal Environments. *Plant Physiol* **134**:1460-1470.
627 Scafaro AP, Xiang S, Long BM, Bahar NHA, Weerasinghe LK, Creek D, Evans JR, Reich
628 PB and Atkin OK (2016) Strong thermal acclimation of photosynthesis in tropical
629 and temperate wet-forest tree species: the importance of altered Rubisco content.
630 *Glob Chang Biol* **23**:2783-2800.
631 Sharkey TD, Bernacchi CJ, Farquhar GD and Singsaas EL (2007) Fitting photosynthetic
632 carbon dioxide response curves for C3 leaves. *Plant Cell Environ* **30**:1035-1040.
633 Silim S, Ryan N and Kubien D (2010) Temperature responses of photosynthesis and
634 respiration in Populus balsamifera L.: acclimation versus adaptation. *Photosynth*
635 *Res* **104**:19-30.
636 Slot M and Winter K (2017) Photosynthetic acclimation to warming in tropical forest tree
637 seedlings. *J Exp Bot* 68:2275-2284.
638 Théroux-Rancourt G, Éthier G and Pepin S (2014) Threshold response of mesophyll CO_2
639 conductance to leaf hydraulics in highly transpiring hybrid poplar clones exposed
640 to soil drying. *J Exp Bot* **65**:741-753.
641 Tjoelker MG, Reich PB and Oleksyn J (1999) Changes in leaf nitrogen and carbohydrates
642 underlie temperature and CO_2 acclimation of dark respiration in five boreal tree
643 species. *Plant Cell Environ* **22**:767-778.
644 TurnbulL M H, Murthy R and Griffin KL (2002) The relative impacts of daytime and night-
645 time warming on photosynthetic capacity in Populus deltoides. *Plant Cell Environ*
646 **25**:1729-1737.
647 von Caemmerer S and Evans JR (2015) Temperature responses of mesophyll conductance
648 differ greatly between species. *Plant Cell Environ* **38**:629-637.
649 Wang D, Li X-F, Zhou Z-J, Feng X-P, Yang W-J and Jiang D-A (2010) Two Rubisco
650 activase isoforms may play different roles in photosynthetic heat acclimation in the
651 rice plant. *Physiol Plant* **139**:55-67.
652 Warren CR (2008) Does growth temperature affect the temperature responses of
653 photosynthesis and internal conductance to CO_2? A test with *Eucalyptus regnans*.
654 *Tree Physiol* **28**:11-19.
655 Way DA and Yamori W (2014) Thermal acclimation of photosynthesis: on the importance
656 of adjusting our definitions and accounting for thermal acclimation of respiration.
657 *Photosynth Res* **119**:89-100.
658 Weston DJ, Bauerle WL, Swire-Clark GA, Moore Bd and Baird WV (2007)
659 Characterization of Rubisco activase from thermally contrasting genotypes of Acer
660 rubrum (Aceraceae). *Am J Bot* **94**:926-934.
661 Yamori W, Hikosaka K and Way DA (2014) Temperature response of photosynthesis in
662 C3, C4, and CAM plants: temperature acclimation and temperature adaptation.
663 *Photosynth Res***119**:101-117.

664 Yamori W, Nagai T and Makino A (2011) The rate-limiting step for CO_2 assimilation at
665 different temperatures is influenced by the leaf nitrogen content in several C3 crop
666 species. *Plant Cell Environ* **34**:764-777.
667 Yamori W, Noguchi K, Hikosaka K and Terashima I (2009) Cold-tolerant crop species
668 have greater temperature homeostasis of leaf respiration and photosynthesis than
669 cold-sensitive species. *Plant Cell Physiol* **50**:203-215.
670 Yamori W, Noguchi K, Kashino Y and Terashima I (2008) The role of electron transport
671 in determining the temperature dependence of the photosynthetic rate in spinach
672 leaves grown at contrasting temperatures. *Plant Cell Physiol* **49**:583-591.
673 Yamori W and von Caemmerer S (2009) Effect of rubisco activase deficiency on the
674 temperature response of CO_2 assimilation rate and rubisco activation state: Insights
675 from transgenic tobacco with reduced amounts of rubisco activase. *Plant Physiol*
676 **151**:2073-2082.

677 Yamori W, Suzuki K, Noguchi K, Nakai M and Terashima I (2006) Effects of rubisco
678 kinetics and rubisco activation state on the temperature dependence of the
679 photosynthetic rate in spinach leaves from contrasting growth temperatures. *Plant*
680 *Cell Physiol* **29**:1659-1670.

681

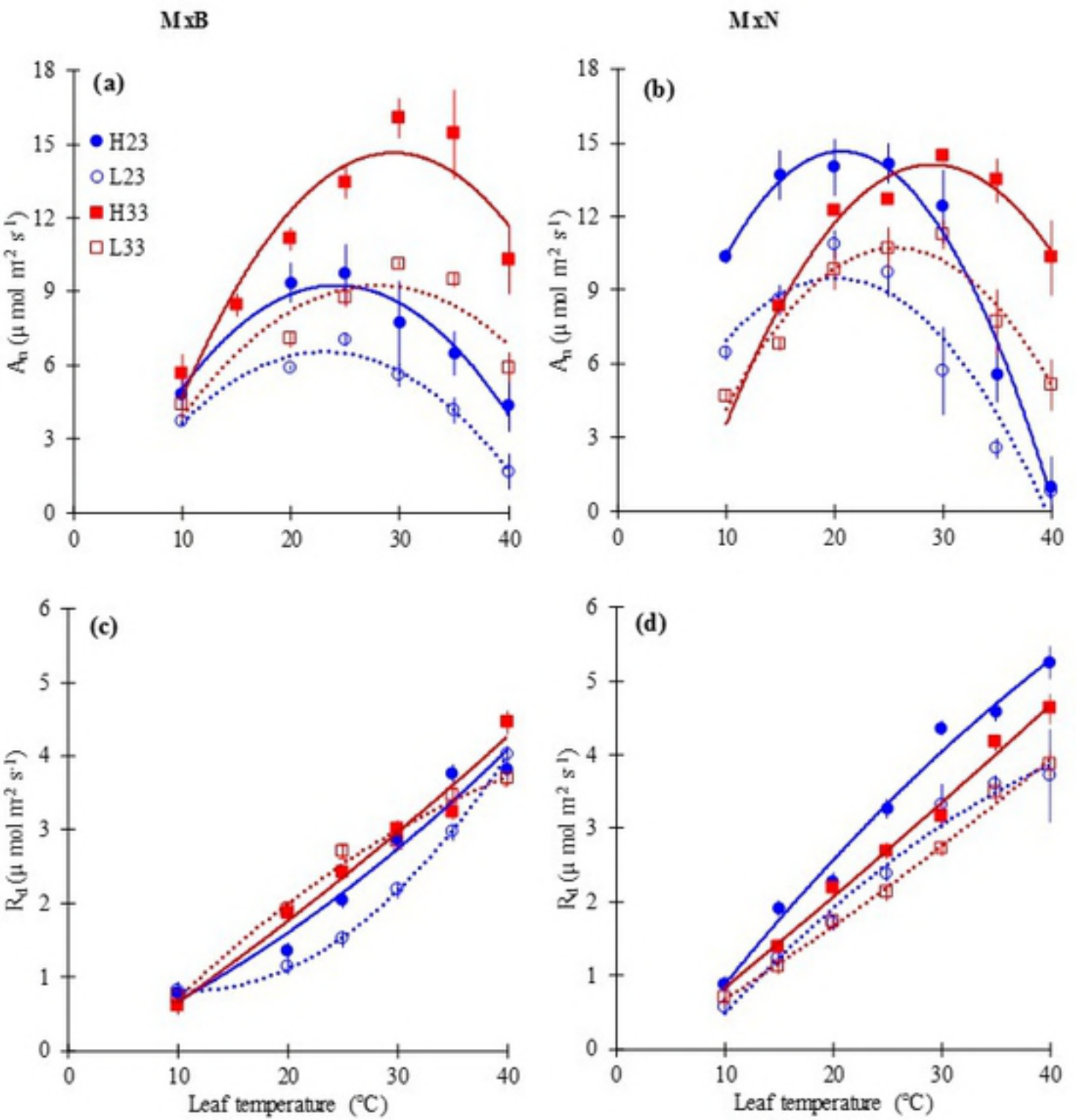
MxB
MxN
(a)
(b)
(c)
(d)
H23
L23
H33
L33
A_n (μ mol m^{-2} s^{-1})
R_d (μ mol m^{-2} s^{-1})
Leaf temperature (°C)
Leaf temperature (°C)

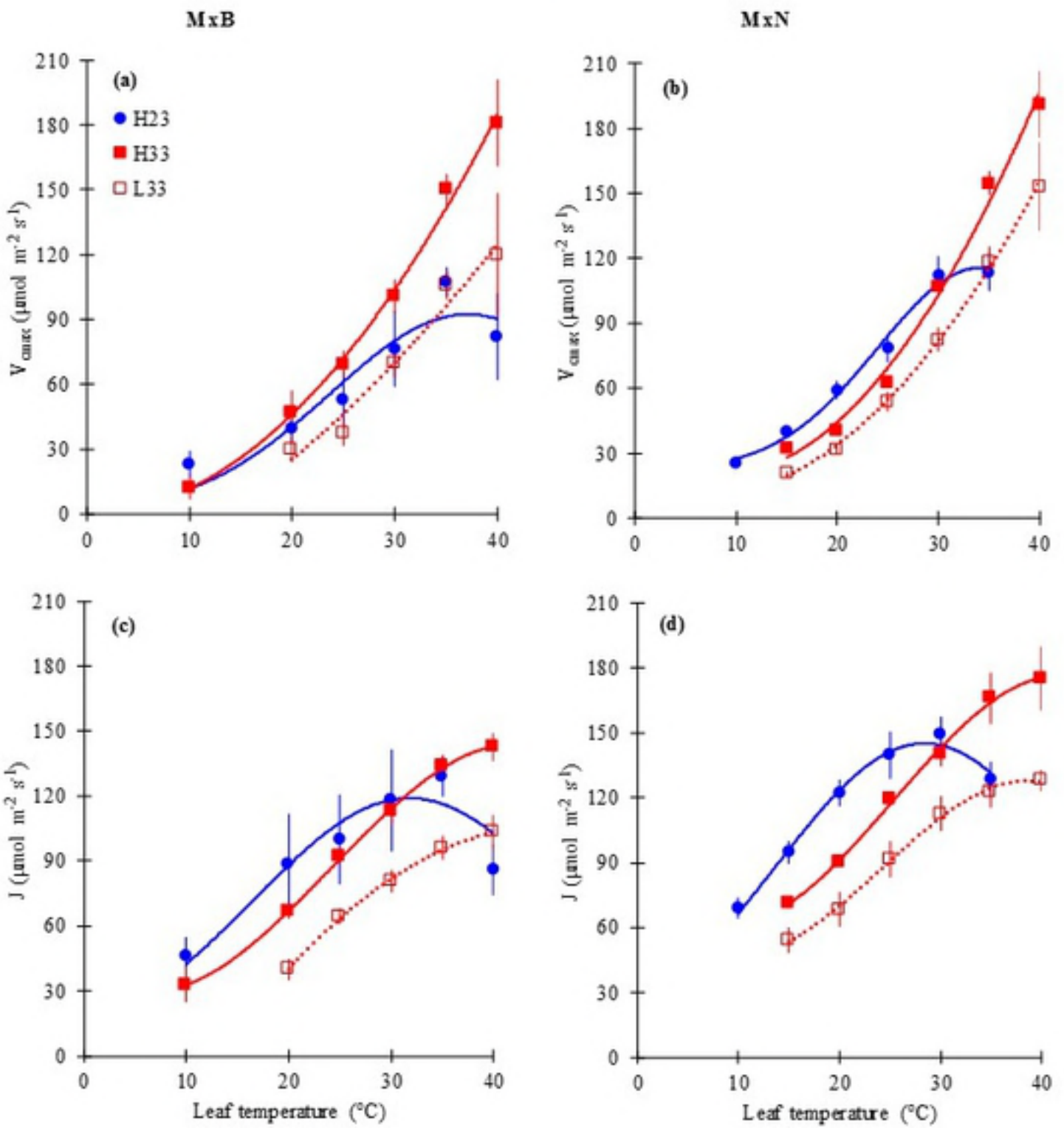
MxB
MxN
(a)
(b)
(c)
(d)
H23
H33
L33
V_{cmax} (µmol m^{-2} s^{-1})
J (µmol m^{-2} s^{-1})
Leaf temperature (°C)
0
30
60
90
120
150
180
210
10
20
30
40

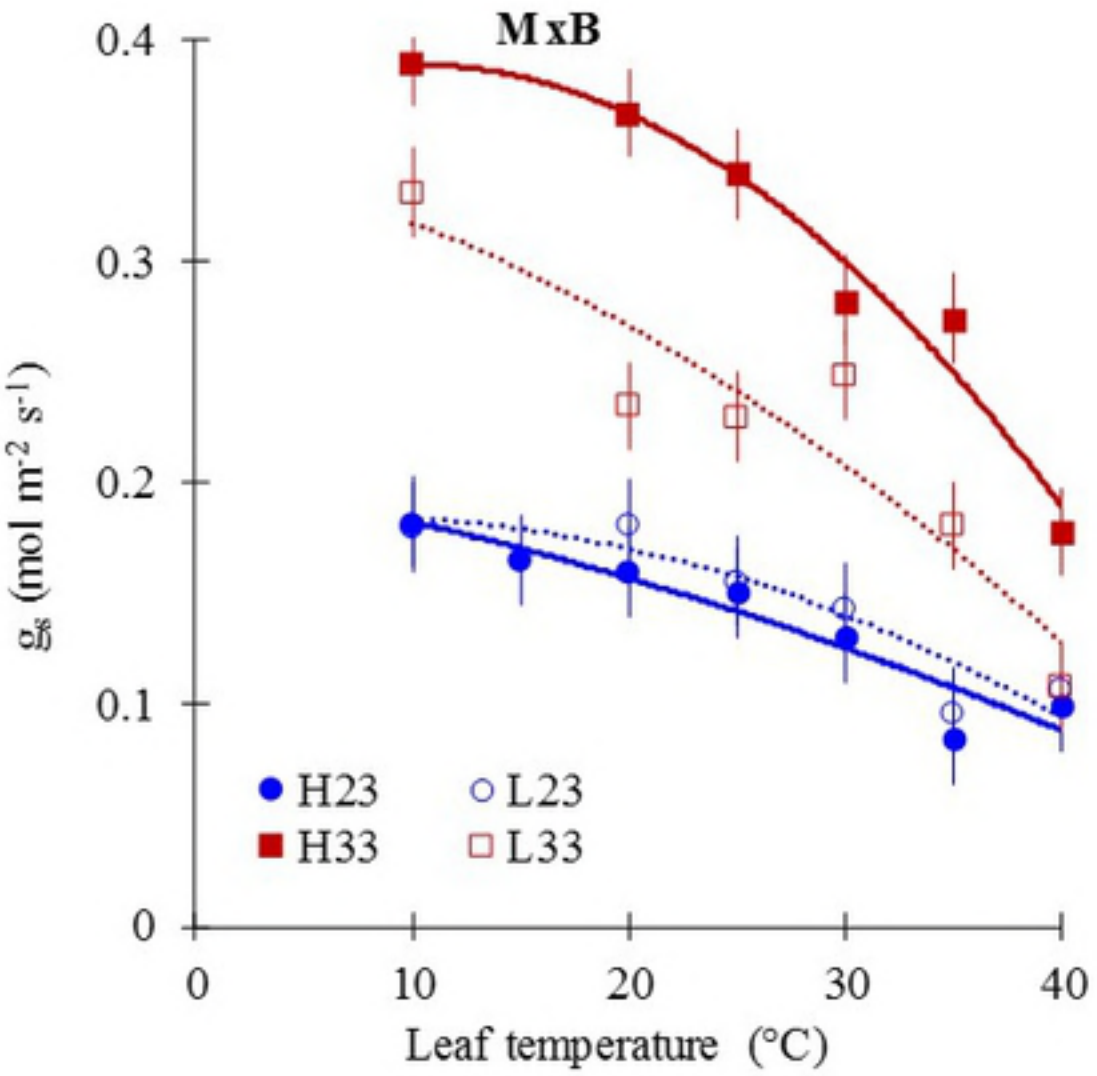
MxB
0.4
0.3
0.2
0.1
0
g_s (mol m^{-2} s^{-1})
H23
L23
H33
L33
0
10
20
30
40
Leaf temperature (°C)

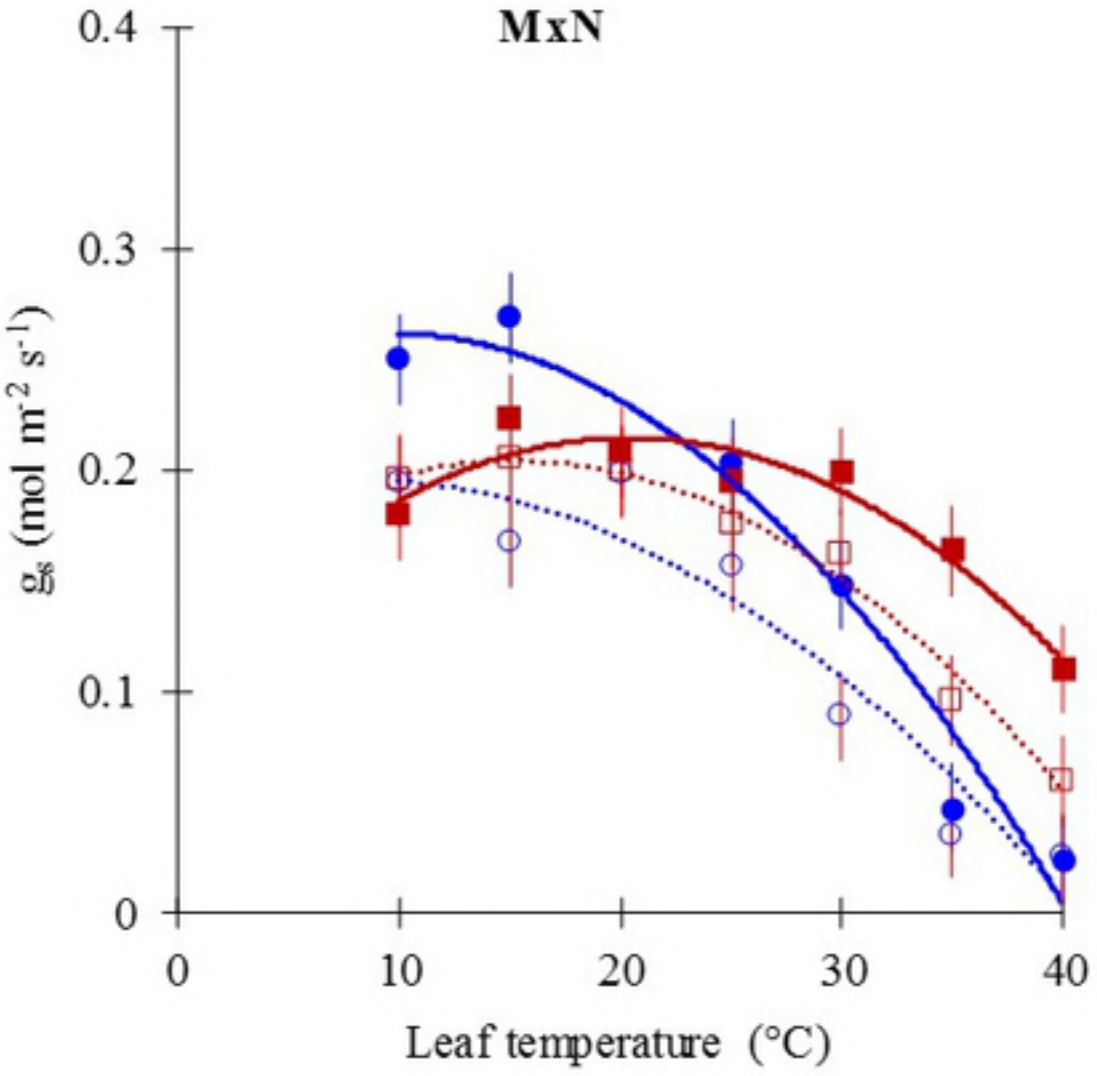
MxN
0.4
0.3
0.2
0.1
0
g_s (mol m^{-2} s^{-1})
0
10
20
30
40
Leaf temperature (°C)

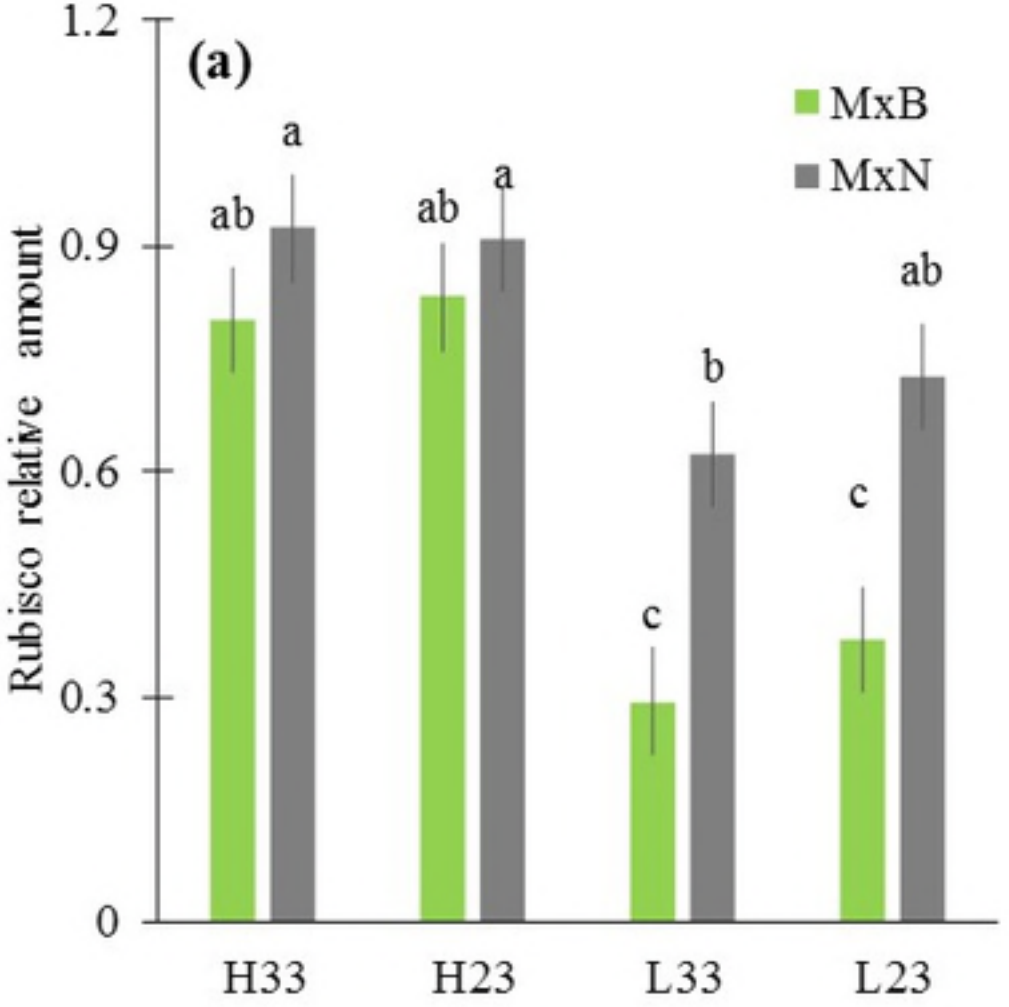
(a)
MxB
MxN
Rubisco relative amount
1.2
0.9
0.6
0.3
0
ab
a
ab
a
c
b
c
ab
H33
H23
L33
L23

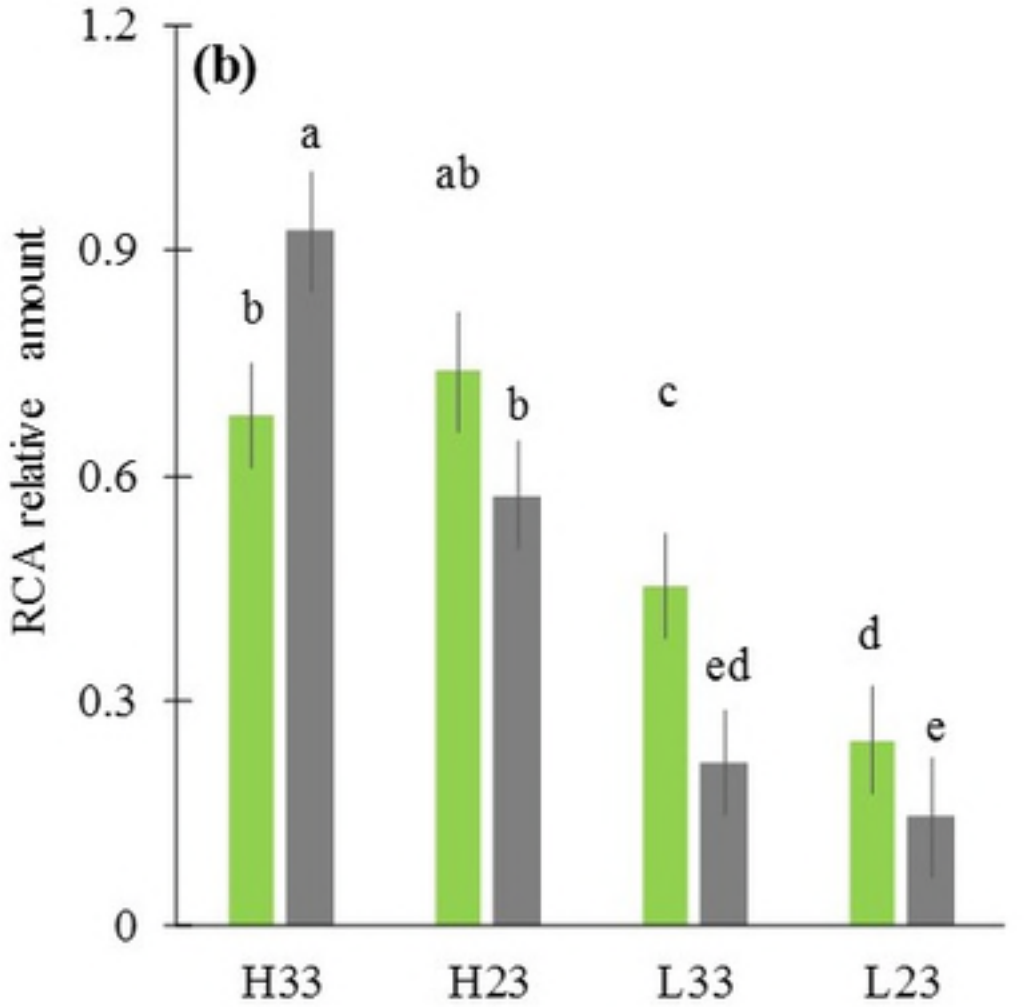
(b)
RCA relative amount
1.2
0.9
0.6
0.3
0
b
a
ab
b
c
ed
d
e
H33
H23
L33
L23

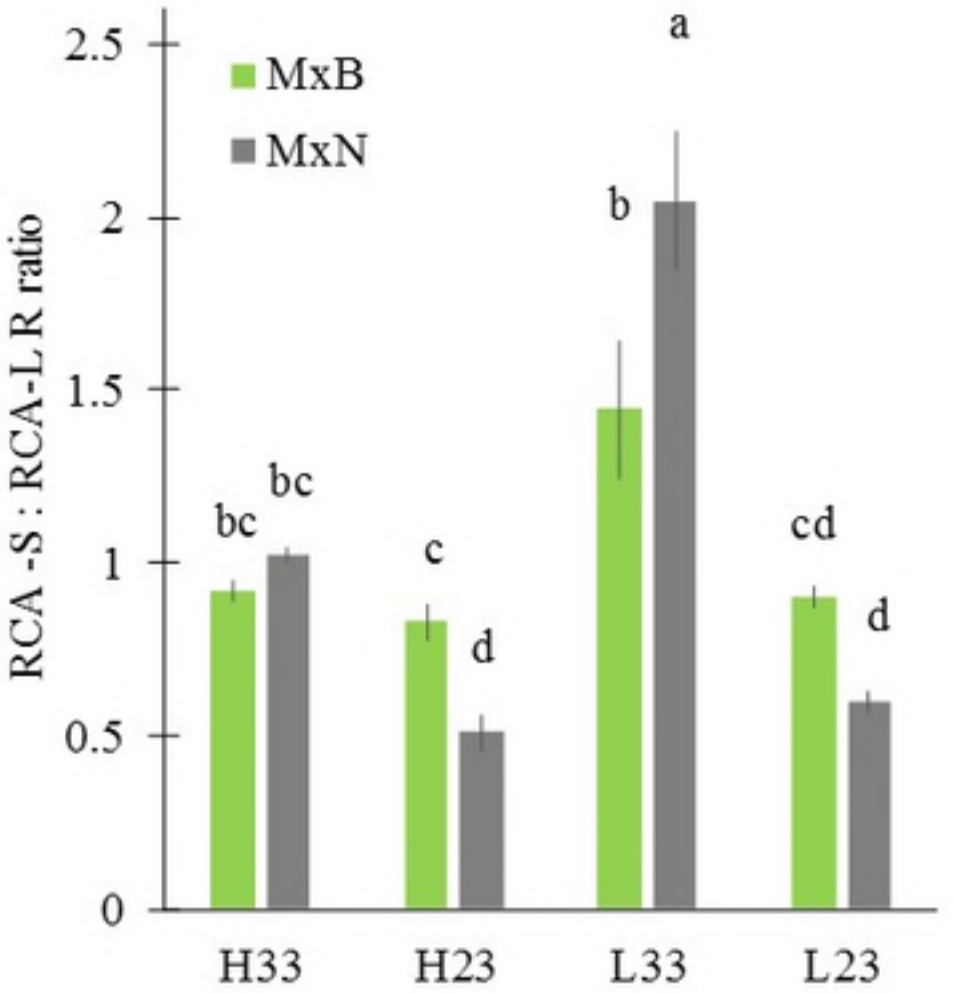
RCA -S : RCA-L R ratio
2.5
2
1.5
1
0.5
0
MxB
MxN
bc
bc
c
d
b
a
cd
d
H33
H23
L33
L23